

# Analysis of Signals with Fast-Varying Instantaneous Frequency: Window Selection and Insights from Synchrosqueezing Transform

Yae-lin Sheu, Liang-Yan Hsu, and Hau-tieng Wu

**Abstract**—We develop a theory for analyzing a signal that consists of multiple oscillatory components with fast-varying instantaneous frequencies. In order to describe this kind of signals, the adaptive harmonic model is extended to include fast-varying instantaneous frequency components. Moreover, we apply the Rényi entropy to measure the time-frequency representation provided by synchrosqueezing transform and determine an optimal window width. For a signal with multiple components, which induce coupling artifacts, we propose an adaptive optimal window approach by segmenting the signal into several sections. Examples presented include a synthetic signal and an application to attosecond physics considering the atomic time-varying dipole moment driven by a two-color midinfrared laser fields.

**Index Terms**—Fast varying instantaneous frequency, synchrosqueezing transform, Rényi entropy, high-harmonic generation.

## I. INTRODUCTION

OSCILLATION reflects not only the system profiles but also how the system interacts with others. While a signal serves as a portal to the system, investigation of the oscillatory behavior of the signal is a fundamental subject. It is well known that Fourier transform is not suitable for studying nonstationary dynamics, despite the fact that it has been widely applied to many fields. As a result, time-frequency (TF) analysis, providing the time-frequency representation (TFR) of the signal, was developed to solve this issue [1], and dynamics of the system can be interpreted from the TFR, if ideally constructed.

During the past 70 years, several TF analysis methods have been developed, including linear-type transforms, quadratic-type transforms, and reassignment methods (RM) [1]. While capturing the dynamics by these methods, disadvantages accompany. Linear-type transforms, such as short time Fourier transform (STFT), are subject to the limitation of Heisenberg uncertainty principle. Quadratic-type transforms, for example, Wigner-Ville distribution, suffer from severe mode mixing artifacts. Although the conventional RMs [2] provide a “sharpened” version of either linear-type or quadratic-type transforms, no inverse transforms are available.

Y.-L. Sheu is with Center for Quantum Science and Engineering, and Center for Advanced Study in Theoretical Sciences, Department of Physics, National Taiwan University, Taipei 10617, Taiwan

L.-Y. Hsu is with Department of Chemistry, Princeton University, Princeton, New Jersey 08544, USA

H. T. Wu is with the Department of Mathematics, University of Toronto, Toronto ON M5S 2E4, Canada. e-mail: (hauwu@math.toronto.edu)

Recently, synchrosqueezing transform (SST) [3], [4] is proposed to alleviate these issues. Based on a chosen linear-type transform, e.g. STFT, SST, as a special case of RMs, manifests “sharpened” oscillatory characteristics according to the reallocation rule that considers solely the phase information of that linear-type transform. In addition, SST preserves the causality property of the signal, leading to an inverse transform. For a signal consists of several oscillatory components, SST provides an adaptive denoise scheme and a mean to extract these oscillatory components.

While SST has been adopted in different fields, ranging from medicine, geography to physics [5]–[11], there are two commonly encountered problems when SST is applied. First, while it is shown theoretically that the TFR determined by SST is not dominantly dependent on the chosen window, the fine details of the TFR is definitely impacted. As a result, how to choose an optimal window based on particular criteria becomes a crucial issue. Second, when the oscillatory signal has a “fast-varying” instantaneous frequency (IF), the choice of window width becomes nontrivial. Since these issues are rooted in STFT or other linear-type transforms, a second-order reallocation rule for SST (second-order SST) [12] or the conventional reassignment techniques also have similar limitations as SST – a poorly chosen window would lead to a poor TFR.

In this letter, continuing our previous theoretical work in SST [3], [4], we report a study on how the window influence SST in case of fast-varying IF components. In short, the SST, as well as second-order SST and RMs, can operate as well by decreasing the window width. With the need of a short window in recent literature [11], [13], we propose a method of how to find an optimal window width by adopting the Rényi entropy [14], which measures how the TFR spreads. In addition to the mathematical theory, we present two examples using synthetic data and simulated atomic time-varying dipole moment driven by a two-color midinfrared laser field [10], [15].

## II. ADAPTIVE HARMONIC MODEL AND SYNCHROSQUEEZING TRANSFORM

To describe the time-varying oscillatory dynamics in a given signal, in particular components with fast varying instantaneous frequencies, we consider the following adaptive harmonic model.

**Definition II.1.** Fix  $0 \leq \epsilon \ll 1$ ,  $c_2 > c_1 > \epsilon$ ,  $c_2 > c_3 > \epsilon$  and  $d > 0$ . Consider a functional set  $\mathcal{Q}_{\epsilon,d}^{c_1,c_2,c_3} \subset$

$C^1(\mathbb{R}) \cap L^\infty(\mathbb{R})$ , which consists of  $x(t) = \sum_{k=1}^K f_k(t) \chi_{I_k}$ , where  $I_k \subset \mathbb{R}$ ,  $|I_k| \gg 1$ ,  $\chi$  is the indicator function, and  $f_k(t) = a_k(t) \cos(2\pi\phi_k(t))$  satisfies for  $k = 1, \dots, K$

$$\begin{cases} a_k(t) \in C^1(\mathbb{R}) \cap L^\infty(\mathbb{R}), \phi_k \in C^3(\mathbb{R}), \\ \inf_{t \in \mathbb{R}} a_k(t) \geq c_1, \inf_{t \in \mathbb{R}} \phi'_k(t) \geq c_1, \\ \sup_{t \in \mathbb{R}} a_k(t) \leq c_2, \sup_{t \in \mathbb{R}} \phi'_k(t) \leq c_2, \\ \sup_{t \in \mathbb{R}} |\phi''_k(t)| \leq c_3, |a'_k(t)| \leq \epsilon \phi'(t) \text{ for all } t \in \mathbb{R}, \end{cases}$$

and for  $k = 2, \dots, K$ ,  $\phi'_k(t) - \phi'_{k-1}(t) > d$ . We could call  $\mathcal{Q}_{\epsilon, d}^{c_1, c_2, c_3}$  the *adaptive harmonic model*,  $f_k$  the  $k$ -th intrinsic mode type (IMT) function of  $x(t)$  and  $a_k(t)$  the *amplitude modulation* (AM) and  $\phi'_k(t)$  the *instantaneous frequency* (IF) of the  $k$ -th IMT function.

Note that most time series we acquire in the real world are real, so we only consider real oscillatory signals in  $\mathcal{Q}_{\epsilon, d}^{c_1, c_2, c_3}$ . Further, in practice the oscillatory components can be intermittent, and  $I_k$  indicates the interval where the  $k$ -th IMT function exists. We say that the  $k$ -th IMT function has the *dynamical existence* when  $I_k \neq \mathbb{R}$ . For discussions about this model, like well-definedness of AM and IF and the identifiability issue, we refer the reader with interest to [16], [17].

SST is proposed to study the adaptive harmonic model. While there are many SSTs embedded on different transforms, such as continuous wavelet transform [3], wave packet [18] or S-transform [19], here we consider the STFT-based SST. Moreover, we simplify the discussion by choosing the Gaussian function with a standard deviation of  $\sigma > 0$  as the window function, i.e.,  $g_\sigma(t) = \frac{1}{\sqrt{2\pi}\sigma} e^{-\frac{t^2}{2\sigma^2}}$ . The STFT of  $x \in \mathcal{Q}_{\epsilon, d}^{c_1, c_2, c_3}$  with respect to the window  $g_\sigma$  is defined by

$$V_x^{g_\sigma}(u, \eta) = \int_{-\infty}^{\infty} x(t) g_\sigma(t - u) e^{-i2\pi\eta(t-u)} dt, \quad (1)$$

where  $u \in \mathbb{R}$  is the time and  $\eta \in \mathbb{R}^+$  is the frequency. The SST with the resolution  $\alpha > 0$  and threshold  $\gamma \geq 0$  is defined by

$$S_{g_\sigma, x}^{\alpha, \gamma}(u, \xi) = \int_{A_{x, \gamma}(u)} V_x^{g_\sigma}(u, \eta) \frac{1}{\alpha} h\left(\frac{|\xi - \omega_x^\gamma(u, \eta)|}{\alpha}\right) d\eta, \quad (2)$$

where  $A_{x, \gamma}(u) := \{\eta \in \mathbb{R}_+ : |V_x^{g_\sigma}(u, \eta)| > \gamma\}$ ,  $h(t) = \frac{1}{\sqrt{\pi}} e^{-t^2}$ ,  $\alpha > 0$  and  $\omega_x(u, \eta)$  is the *reallocation rule*:

$$\omega_x^\gamma(u, \eta) = \begin{cases} \frac{-i\partial_u V_x^{g_\sigma}(u, \eta)}{2\pi V_x^{g_\sigma}(u, \eta)} & \text{when } |V_x^{g_\sigma}(u, \eta)| \geq \gamma \\ -\infty & \text{when } |V_x^{g_\sigma}(u, \eta)| < \gamma. \end{cases} \quad (3)$$

In a nutshell, the TFR determined by STFT is sharpened by reassigning its coefficient at  $(u, \eta)$  to a different point  $(u, \xi)$  according to a reallocation rule. Note that the reassignment process in SST a nonlinear operation.

### III. SMALL WINDOW IN SST

We show that when the window width is adequately small and when the IFs of oscillatory components are separated far enough, SST could provide a sharp TFR.

Define universal constants  $I_l := \int |t|^l |g(t)| dt$ , where  $k, l \in \mathbb{N} \cup \{0\}$ .

**Theorem III.1.** Take  $x(t) = \sum_{k=1}^K a_k(t) \cos(2\pi\phi_k(t)) \chi_{I_k} \in \mathcal{Q}_{\epsilon, d}^{c_1, c_2, c_3}$  and fix  $u \in \mathbb{R}$ . Take  $0 < \sigma \ll 1$  and suppose  $d > \frac{\sqrt{-\log \epsilon}}{\sqrt{2\pi}\sigma}$ . Denote  $I_k = (\alpha_k, \beta_k) \subset \mathbb{R}$ ,  $\mathcal{Z}_k := \{(u, \eta) : |\eta - \phi'_k(u)| < d/2\}$  and the boundary area  $B_x := [(\cup_{k=1}^K, \alpha_k \neq -\infty [\alpha_k - \sqrt{\sigma}, \alpha_k + \sqrt{\sigma}]) \cup (\cup_{k=1}^K, \beta_k \neq \infty [\beta_k - \sqrt{\sigma}, \beta_k + \sqrt{\sigma}])] \times \mathcal{Z}_k$ . By taking the window width as  $\sigma$ , as  $\sigma$  is small enough, we have for all  $(u, \eta) \in \mathbb{R} \times \mathbb{R}^+ \setminus B_x$ ,

$$|V_x^{g_\sigma}(u, \eta) - V_{x(u)}^{g_\sigma}(u, \eta)| \leq \Gamma_1(\epsilon, \sigma), \quad (4)$$

$$|\partial_u V_x^{g_\sigma}(u, \eta) - 2\pi i \phi'_k(u) V_{x(u)}^{g_\sigma}(u, \eta)| \leq \Gamma_2(\epsilon, \sigma), \quad (5)$$

where  $x_{(u)}(t) := \sum_{k=1}^K a_k(u) \cos(2\pi(\phi_k(u) + \phi'_k(u)(t - u))) \chi_{I_k}$ ,

$$\Gamma_1(\epsilon, \sigma) := K c_2 [2\pi c_3 \sigma I_2 + \sigma^2 + \epsilon I_1] \sigma \quad (6)$$

$$\Gamma_2(\epsilon, \sigma) := K c_2 [\epsilon (2\pi c_2 \sigma + 1) I_1 + 2\pi c_3 \sigma (I_1 + c_2 I_2 \sigma) + 2\pi(\epsilon + \sigma^3)].$$

Further, for all  $\eta \in \mathbb{R}^+ \setminus (\cup_{k=1}^K, u \in (\alpha_k + \sqrt{\sigma}, \beta_k - \sqrt{\sigma}) \mathcal{Z}_k)$ ,

$$|V_{x(u)}^{g_\sigma}(u, \eta)| \leq K c_2 (\sigma^3 + \epsilon). \quad (7)$$

The proof of Theorem III.1 is provided in Appendix A. The main difference between the proof of Theorem III.1 and that in [3] is that we take the window length into account to reduce the error caused by the fast varying IF. Note that in [3] the IF is assumed to vary slowly; that is,  $c_2 = O(\epsilon)$ . Theorem III.1 suggests that when we apply SST to the adaptive harmonic model,  $V_x^{g_\sigma}(u, \eta)$  is concentrated only near the IFs  $\phi'_k(u)$  with the error of order  $\epsilon^{1/3}$ , and the dominant error term depends on  $c_3$ , which describes how fast the IF varies. In  $\mathcal{Q}_{\epsilon, d}^{c_1, c_2, c_3}$ , in which the IF can vary fast, we have to choose a small window in order to control the error caused by the fast-varying IF; that is, the term  $c_3 \sigma$  in both  $\Gamma_1(\epsilon, \sigma)$  and  $\Gamma_2(\epsilon, \sigma)$ . Note that  $x_{(u)}$  in Theorem III.1 is a harmonic function, which well approximates  $x$  near  $u$ . With Theorem III.1, it is straight forward to show that with the small window, the reallocation rule Eq. (3) provides the correct IF information and we could accurately reconstruct each oscillatory component.

**Theorem III.2.** With the same notations and assumptions in Theorem III.1, we have that for all  $(t, \eta) \in \mathbb{R} \times \mathbb{R}^+ \setminus B_x$ , when  $|V_x^{g_\sigma}(u, \eta)| \geq \gamma$ ,

$$|\omega_x^\gamma(u, \eta) - \phi'_k(u)| \leq \frac{\Gamma_2(\epsilon, \sigma) + c_2 \Gamma_1(\epsilon, \sigma)}{|V_x^{g_\sigma}(u, \eta)|}, \quad (8)$$

and for each  $k \in \{1, \dots, K\}$ , for any  $u \in [\alpha_k + \epsilon, \beta_k - \epsilon]$ ,

$$|\frac{1}{g(0)} \int_{\mathcal{Z}_k} S_{g_\sigma, x}^{\alpha, \gamma}(u, \eta) \eta - a_k(u) e^{i2\pi\phi_k(u)}| \leq \Gamma_4(\epsilon, \sigma), \quad (9)$$

where  $\Gamma_4$  is a universal constant depending on  $I_l^g$ ,  $l = 0, 1, 2$ ,  $c_1$ ,  $c_2$  and  $c_3$ .

Based on Theorem III.1, the proof of Theorem III.2 is similar to that of Estimate 3.9 in [3], thereby omitted in this letter. As indicated by Eq. (8), the larger  $|V_x^{g_\sigma}(u, \eta)|$  is, the smaller the difference between  $\omega_x^\gamma(u, \eta)$  and  $\phi'_k(u)$ . Note that since  $\omega_x^\gamma(u, \eta)$  or its equivalent variation is a building block of the RM and 2nd-order SST, if SST fails to extract the IF

from the signal, RM and 2nd-order SST might also fail. See the supplementary for examples.

For a real signal  $x(t) = \sum_{k=1}^K a_k(t) \cos(2\pi\phi_k(t))$ , to obtain its complex form is a nontrivial issue [20], [21]. In general, the imaginary counterpart is obtained via Hilbert transform. However, for the signal  $x(t) \in \mathcal{Q}_{\epsilon,d}^{c_1,c_2,c_3}$ , it is not easy to fulfill the conditions for Hilbert transform, and the situation is worsened when any IMT function has the dynamical existence. Hence, obtaining the signal in complex form via Hilbert transform might not be feasible. The inversion formula (9) in this theorem can serve as an alternative method to obtain its complex form, denoted as  $x^{\mathbb{C}}(t) = \sum_{k=1}^K a_k(t) e^{i2\pi\phi_k(t)}$ . According to Theorem III.2, we could approximate  $x^{\mathbb{C}}$  by  $g(0)^{-1} \int_{\cup_{k=1}^K \mathcal{Z}_k} V_x^{g\sigma}(u, \eta) d\eta$ .

Theorems III.1 and III.2 indicate another benefit of applying the small window – finer temporal resolution to extract the dynamical information. Indeed, suppose the  $k$ -th IMT function has dynamical existence. With the small window, we could obtain an accurate information indicating the very instant of appearance and disappearance of the IMT function. In another word, for the  $k$ -th IMT function, except the temporal interval of the window length  $\epsilon$  in  $B_x$ , we could obtain accurate information, even reconstructing the  $k$ -th IMT function.

#### IV. WINDOW CHOICE BY RÉNYI ENTROPY

Theorem III.1 and III.2 indicate that the performance of the SST is improved by decreasing the window width. Nevertheless, there is an extent that the small window cannot catch the IF components and causes severe coupling between different IF components. To determine the best window width, we adopt the measure of the normalized TFR using Rényi entropy [14], [22], [23]. Consider  $\alpha > 0$ , the Rényi entropy is defined as

$$R_\alpha := \frac{1}{1-\alpha} \log_2 \iint \left( \frac{R^{(\sigma)}(t, f)}{\iint R^{(\sigma)}(s, \xi) ds d\xi} \right)^\alpha dt df, \quad (10)$$

where  $R^{(\sigma)}(t, f)$  can be  $|V_x^{g\sigma}(t, f)|$  or  $|S_{g\sigma, x}^{\alpha, \gamma}(t, f)|$  or any other TFR. It has been well known that a larger Rényi entropy leads to less concentration the distribution. Thus, a concentrated TFR could be obtained by finding a window width such that the corresponding Rényi entropy is minimized; that is, the optimal window width is determined by

$$\tilde{\sigma} := \operatorname{argmin}_{\sigma > 0} R_\alpha. \quad (11)$$

In general,  $\alpha > 2$  being values recommended for TFR measures [23]. In this study, we chose  $\alpha = 2$ . In practice, we notice that for results for different  $\alpha > 0$  are slightly worse but acceptable.

#### V. RESULTS

We demonstrate the optimal TFR of the SST can be obtained by minimizing Rényi entropy via controlling the window width. Analyses for a synthetic data and the laser-driven atomic dipole moment are presented.

##### A. Synthetic Signal

The first set of simulations consists of a multicomponent frequency modulated oscillation, given by

$$\begin{aligned} x(t) = & \cos(2\pi\phi_1(t))h(-(t-20)) \\ & + \cos(2\pi\phi_2(t))h(-(t-13.6)) \\ & + \cos(2\pi\phi_3(t))h(t-17.5), \end{aligned} \quad (12)$$

where  $h(t)$  denotes the Heaviside function and the phase functions are

$$\begin{aligned} \phi_1(t) &= e^{(t-5)(\ln 1.33)} + 3t \\ \phi_2(t) &= -0.0437(t-5)^4 + 0.5(t-5)^3 + 0.25(t-5)^2 + 5t \\ \phi_3(t) &= -\frac{2.7}{3.5} \cos(3.5t) + 0.85(t-15)^2 + 0.5t. \end{aligned}$$

The corresponding instantaneous frequencies are  $\phi'_1(t) = (\ln 1.33)1.33^{(t-5)} + 3$ ,  $\phi'_2(t) = -0.175(t-5)^3 + 1.5(t-5)^2 + 0.5(t-5) + 5$  and  $\phi'_3(t) = 2.7\sin 3.5t + 1.7(t-15) + 0.5$ . The signal is sampled at 300 Hz for 30 seconds, and the signal-to-noise ratio is 15dB. The Rényi entropy for the  $\sigma$  ranging from 0.023s to 1.62s are shown in Fig. 1(a). The optimal window that minimizes Rényi entropy is 0.056s and the corresponding TFR by the SST is presented in Fig. 1(b), where the TFR values are normalized using the z-score definition. Fig. 1(b) demonstrates that SST along with the optimal window width can well describe IFs with the exponential and polynomial growth rate, and sinusoidal variation. We mention that there is a trade-off between the concentration of the IF components on the TFR and the ability to distinguish neighboring components. For example, at the time 5s, the gap between the nearest components are 1.8 Hz. According to Theorems III.1, the window width, measured by full width at half maximum (FWHM) and  $\text{FWHM} = 2\sqrt{2\ln 2}\sigma$ , to separate the two components need to be at least  $1/1.8 \approx 0.55$ s. However, the FWHM of the chosen optimal window is 0.13s, and results in coupling of the two components. Similar disturbance on the IF of  $\phi_1(t)$  can be seen at time 13.6, and 18.5s, where the gaps are 3 and 7 Hz, respectively. Optimal windows for STFT, second-order SST, and reassignment method are discussed in supplementary material.

Clearly, the optimal window based on the Rényi entropy leads to a sharper TFR, since the Rényi entropy balances the coupling artifact between closing IF components and the diffusion caused by the fast-varying IF components. However, as it is defined globally, the chosen optimal window could not well capture the local details. In order to further improve the TFR qualify, we could consider the following *adaptive optimal window* approach – divide the signal into  $L$  overlapping (or non-overlapping) segments, and find the optimal window for each segment. The TFR for the whole signal is synthesized using the results with these optimal windows. The result of this approach, with  $L = 3$  non-overlapping segments, is shown in Fig. 2. The three segments are [0, 10]s, [6, 18]s, and [14, 25]s, and the corresponding  $\sigma$ s are 0.128s, 0.083s, and 0.050s, respectively. Although the FWHM of the chosen optimal window for the first segment is 0.301s, which is smaller than the required 0.55s for a full separation, the artifact

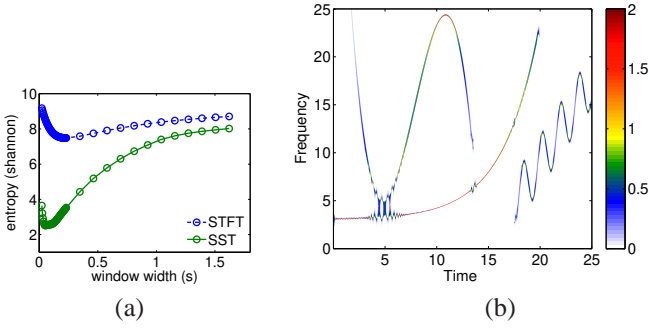


Fig. 1. (a) Rényi entropy of the TFR of a synthetic signal determined by the SST versus window width. (b) The TFR of a synthetic signal determined by the SST using the window width that minimizes the Rényi entropy.

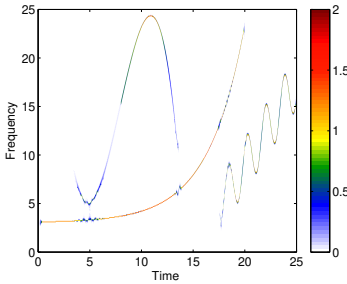


Fig. 2. The TFR of the synthetic signal determined by the SST with the time-varying window approach based on the Rényi entropy.

is lessened at the price of broadening of the fast-varying IF branch ranging from 0 to 4s.

### B. Application to Attosecond Physics

During the past decade, real-time observation and direct control of electronic motion in atoms, molecules, nanostructures and solids have been achieved due to advent in synthesis of attosecond pulses [24]. In general, an isolated attosecond pulse is created by superposition of a broadband supercontinuum in high-order harmonic generation driven by a high-intensity femtosecond laser pulses [25]. To date, an isolated attosecond pulse as short as 67 attosecond has been reported [26]. To synthesize shorter attosecond pulses, a better understanding of the underlying physical mechanism is needed. The physical mechanism of synthesis of attosecond pulses can be understood by analyzing the electron dipole moment oscillation induced by an applied laser field via time-frequency analysis. In previous literature [13], [27], linear-type transform based on short windows has been adopted and the results are consistent with classical trajectory simulations [28]; yet, there is no discussion on how and why small windows are chosen in the field of attosecond physics.

To clarify this issue, we consider a case of the electron dipole moment in atomic hydrogen evoked by an optimally shaped laser waveform that can generate an isolated 21 attosecond pulse [15]. Such laser profile can greatly extend the high-order harmonics up to 900 harmonics within a short time interval, suggesting very fast-varying IF components. The time-

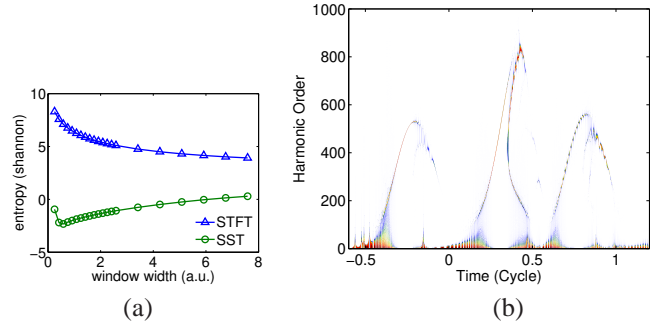


Fig. 3. (a) Rényi entropy of the TFR of the electron dipole moment in acceleration form. (b) The TFR of using the optimal window with the least Rényi entropy. The second emission that reaches up to the 900th harmonic order in a very short interval can be utilized to synthesize an isolated ultrashort attosecond pulse.

dependent dipole moment in acceleration form is computed by solving three-dimensional time-dependent Schrödinger equation in the framework of the time-dependent generalized pseudospectral (TDGPS) method within the electric dipole approximation [29]. The TDFPS method gives high accuracy of orbital energies and has been employed in strong field physics as well as attosecond science. The simulation details are referred to [15].

Next, we compute the Rényi entropy for a series of window width, as shown in Fig. 3(a). The window width that minimizes the entropy is found to be 1.4 atomic unit (a.u.). The corresponding TFR by the SST is presented in Fig. 3(b). Figure 3(b) indicates that there are three emissions taking place. The cutoffs of the first and third emissions are located at around the 500th order, and the second emission reaches the 900th order. The branches on the TFR nearly coincide with classical trajectories reported in the previous literature [15].

It is observed that the branch located around 0.35 a.u., which corresponds to the long trajectory quantum path, has the strongest intensity and consists of the most harmonics. More importantly, these high order harmonics occur almost simultaneously, which is a prerequisite of a dependable attosecond pulse.

## VI. CONCLUSION

We study the adaptive harmonic model that comprises fast-varying IF components by the SST, and theoretically we show that a small window width is preferred in order to capture the fast-varying IF components. To obtain the optimal window width, we consider minimizing the Rényi entropy of the TFR. The performance of the proposed method has been demonstrated on both a synthetic signal and a physical observable. In addition, we demonstrate how the idea of adaptive optimal window helps improve the TFR quality.

## VII. ACKNOWLEDGEMENT

Hau-tieng Wu acknowledges the support of Sloan Research Fellow FR-2015-65363. Yae-lin Sheu appreciates Y. Chou for her advice on numerical parameters of the generalized pseudospectral method.



## REFERENCES

- [1] P. Flandrin, *Time-frequency / time-scale analysis*. Academic Press, 2008.
- [2] E. Chassande-Mottin, F. Auger, and P. Flandrin, "Time-frequency/time-scale reassignment," in *Wavelets and signal processing*, ser. Appl. Numer. Harmon. Anal. Boston, MA: Birkhäuser Boston, 2003, pp. 233–267.
- [3] I. Daubechies, J. Lu, and H.-T. Wu, "Synchrosqueezed wavelet transforms: An empirical mode decomposition-like tool," *Appl. Comput. Harmon. Anal.*, vol. 30, pp. 243–261, 2011.
- [4] H.-T. Wu, "Adaptive Analysis of Complex Data Sets," Ph.D. dissertation, Princeton University, 2011.
- [5] H.-T. Wu, Y.-H. Chan, Y.-T. Lin, and Y.-H. Yeh, "Using synchrosqueezing transform to discover breathing dynamics from ecg signals," *Appl. Comput. Harmon. Anal.*, vol. 36, pp. 354–359, 2014.
- [6] H.-T. Wu, S.-S. Hseu, M.-Y. Bien, Y. R. Kou, and I. Daubechies, "Evaluating physiological dynamics via synchrosqueezing: Prediction of ventilator weaning," *IEEE Trans. Biomed. Eng.*, vol. 61, pp. 736–744, 2013.
- [7] Y.-T. Lin, H.-T. Wu, J. Tsao, H.-W. Yien, and S.-S. Hseu, "Time-varying spectral analysis revealing differential effects of sevoflurane anaesthesia: non-rhythmic-to-rhythmic ratio," *Acta Anaesthesiologica Scandinavica*, vol. 58, pp. 157–167, 2014.
- [8] R. H. Herrera, J. Han, and M. van der Baan, "Applications of the synchrosqueezing transform in seismic time-frequency analysis," *Geophysics*, vol. 79, no. 3, pp. V55–V64, 2014.
- [9] Y.-I. Sheu, L.-Y. Hsu, H.-t. Wu, P.-C. Li, and S.-I. Chu, "A new time-frequency method to reveal quantum dynamics of atomic hydrogen in intense laser pulses: Synchrosqueezing transform," *AIP Advances*, vol. 4, no. 11, 2014. [Online]. Available: <http://scitation.aip.org/content/aip/journal/adva/4/11/10.1063/1.4903164>
- [10] Y.-L. Sheu, H. T. Wu, and L. Y. Hsu, "Exploring laser-driven quantum phenomena from a time-frequency analysis perspective: a comprehensive study," *Opt. Express*, vol. 23, no. 23, pp. 30 459–30 482, Nov 2015.
- [11] P.-C. Li, Y.-L. Sheu, C. Laughlin, and S.-I. Chu, "Dynamical origin of near- and below-threshold harmonic generation of cs in an intense mid-infrared laser field," *Nat. Comm.*, vol. 6, p. 7178, 2015.
- [12] T. Oberlin, S. Meignen, and V. Perrier, "Second-order synchrosqueezing transform or invertible reassignment? towards ideal time-frequency representations," *IEEE Trans. Signal Process.*, vol. 63, no. 5, pp. 1335–1344, March 2015.
- [13] C. C. Chirilă, I. Dreissigacker, E. V. van der Zwan, and M. Lein, "Emission times in high-order harmonic generation," *Phys. Rev. A*, vol. 81, p. 033412, Mar 2010. [Online]. Available: <http://link.aps.org/doi/10.1103/PhysRevA.81.033412>
- [14] R. G. Baraniuk, P. Flandrin, A. J. E. M. Janssen, and O. J. J. Michel, "measuring time-frequency information content using the rényi entropies," *IEEE Trans. Inf. Theory*, vol. 47, no. 4, pp. 1391 – 1049, 2001.
- [15] Y. Chou, P.-C. Li, T.-S. Ho, and S.-I. Chu, "Optimal control of high-order harmonics for the generation of an isolated ultrashort attosecond pulse with two-color midinfrared laser fields," *Phys. Rev. A*, vol. 91, p. 063408, Jun 2015.
- [16] Y.-C. Chen, M.-Y. Cheng, and H.-T. Wu, "Nonparametric and adaptive modeling of dynamic seasonality and trend with heteroscedastic and dependent errors," *J. Roy. Stat. Soc. B*, vol. 76, pp. 651–682, 2014.
- [17] M. Kowalski, A. Meynard, and H.-T. Wu, "Convex Optimization approach to signals with fast varying instantaneous frequency," *ArXiv e-prints 1503.07591*, 2015.
- [18] H. Yang, "Synchrosqueezed Wave Packet Transforms and Diffeomorphism Based Spectral Analysis for 1D General Mode Decompositions," *Appl. Comput. Harmon. Anal.*, vol. 39, pp. 33–66, 2014.
- [19] Z. Huang, J. Zhang, T. Zhao, and Y. Sun, "Synchrosqueezing s-transform and its application in seismic spectral decomposition," *Geoscience and Remote Sensing, IEEE Transactions on*, vol. PP, no. 99, pp. 1–9, 2015.
- [20] A. H. Nuttall, "On the quadrature approximation to the hilbert transform of modulated signals," *Proc. IEEE*, vol. 54, pp. 1458–1459, 1966.
- [21] J. Huang, Y. Wang, and L. Yang, "Vakman's problem and the extension of hilbert transform," *Appl. Comput. Harmon. Anal.*, vol. 34, no. 2, pp. 308 – 316, 2013.
- [22] E. Sejdic, I. Djurovic, and J. Jiang, "Timefrequency feature representation using energy concentration: An overview of recent advances," *Digital Signal Process.*, vol. 19, no. 1, pp. 153 – 183, 2009.
- [23] L. Stankovic, "A measure of some timefrequency distributions concentration," *Signal Process.*, vol. 81, no. 3, pp. 621 – 631, 2001, special section on Digital Signal Processing for Multimedia.
- [24] F. Krausz and M. Ivanov, "Attosecond physics," *Rev. Mod. Phys.*, vol. 81, pp. 163–234, Feb 2009.
- [25] M. Chini, K. Zhao, and Z. Chang, "The generation, characterization and applications of broadband isolated attosecond pulses," *Nature Photon.*, vol. 8, pp. 178–186, Oct 2149.
- [26] K. Zhao, Q. Zhang, M. Chini, Y. Wu, X. Wang, and Z. Chang, "Tailoring a 67 attosecond pulse through advantageous phase-mismatch," *Opt. Lett.*, vol. 37, no. 18, pp. 3891–3893, Sep 2012.
- [27] X. M. Tong and S.-I. Chu, "Probing the spectral and temporal structures of high-order harmonic generation in intense laser pulses," *Phys. Rev. A*, vol. 61, p. 021802, Jan 2000. [Online]. Available: <http://link.aps.org/doi/10.1103/PhysRevA.61.021802>
- [28] P. B. Corkum, "Plasma perspective on strong field multiphoton ionization," *Phys. Rev. Lett.*, vol. 71, pp. 1994–1997, Sep 1993.
- [29] X. M. Tong and S.-I. Chu, "Theoretical study of multiple high-order harmonic generation by intense ultrashort pulsed laser fields: A new generalized pseudospectral time-dependent method," *Chem. Phys.*, vol. 217, no. 2-3, pp. 119 – 130, 1997.